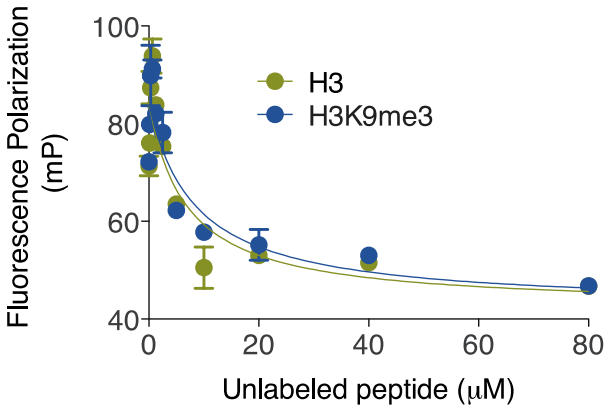

Supplementary Fig. 1 | PHD1 domain binds H3 WT and H3K9me3 tail peptides with a similar affinity. Errors ($n \geq 3$) represent s.e.m.

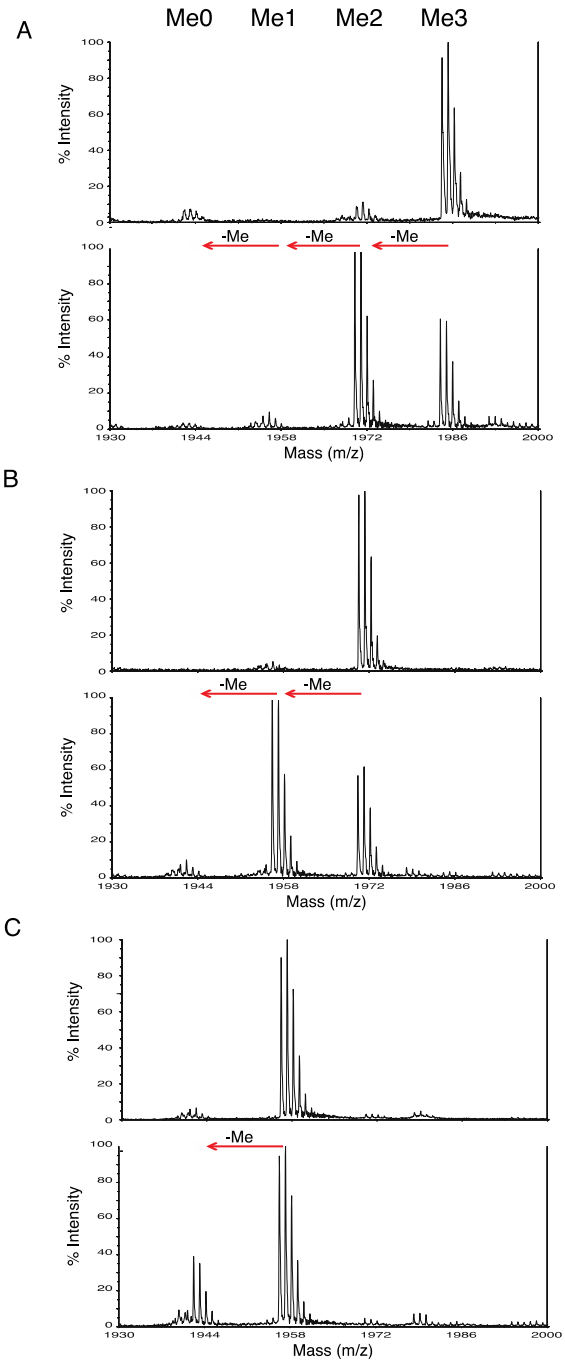

Supplementary Fig. 2 | MALDI analysis of demethylation of **(a)** H3K4me3, **(b)** H3K4me2, and **(c)** H3K4me1 peptides by KDM5A$_{1\text{-}797}$.

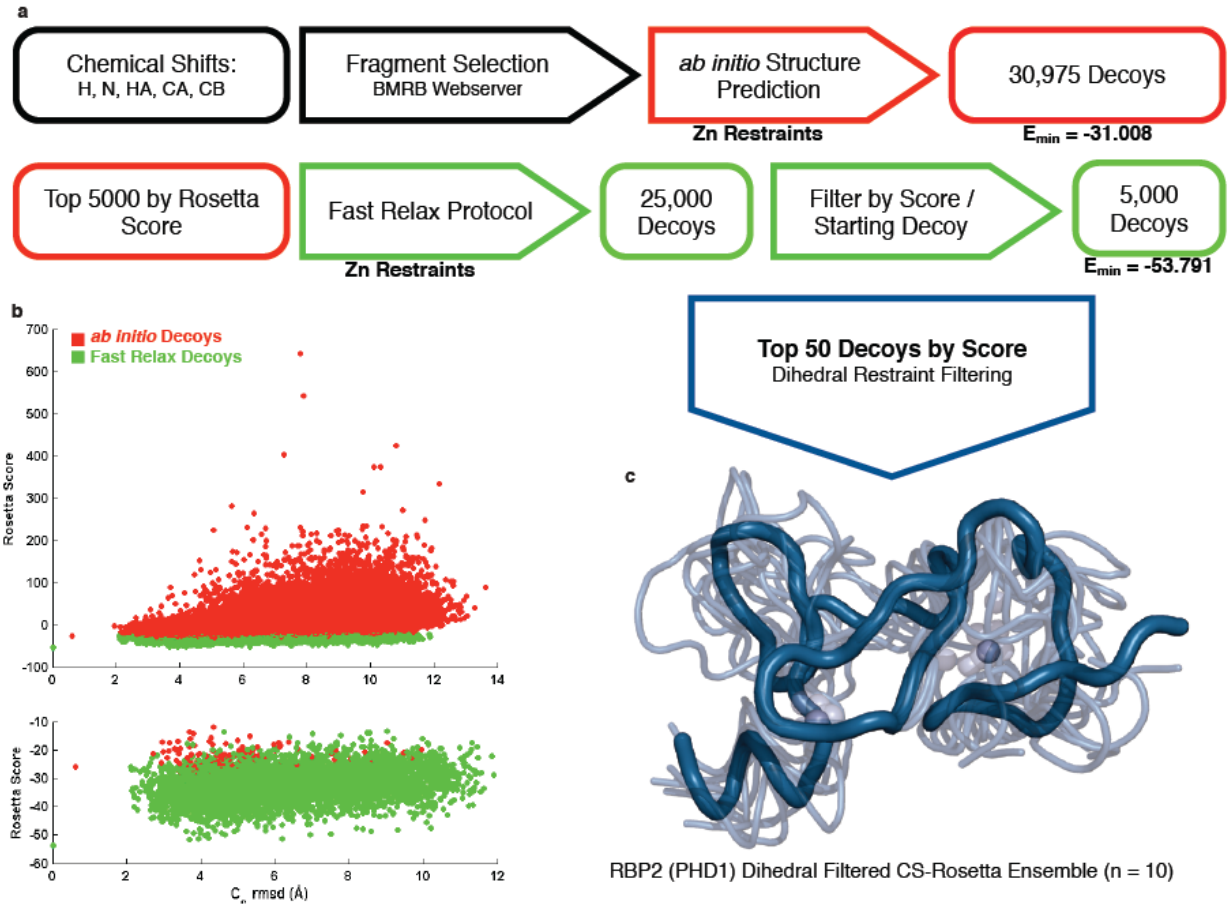

Supplementary Fig. 3 | Flow chart and all-Cα score / rmsd for the CS-Rosetta modeling of the apo KDM5A PHD1. (**a**), Fragments (3-mer and 9-mer) for Rosetta *ab initio* structure prediction were generated using the BMRB webserver. These fragments were then used in Rosetta (v 3.5) *ab initio* structure prediction calculations incorporating appropriate zinc coordination restraints. At the *ab initio* stage, 30,975 decoys were generated. The top 5,000 decoys by Rosetta Score were then selected for additional refinements using a fast relax protocol that generated a total of 25,000 new decoys. These were filtered by score and starting decoy identity. The top 50 decoys were then filtered using the dihedral restraint violations viewer within CCPNMR. Only models with dihedral violations less than 15^{o} were included in the final ensemble. (**b**), In the score /

rmsd plot, models from the *ab initio* structure prediction are indicated with a red circle and those with the additional fast relax protocol are indicated with a green circle. (**c**), The dihedral filtered ensemble (n=10) is drawn as ribbons with the lowest scoring CS-Rosetta decoy and the model used in the main text indicated by the thicker ribbon.

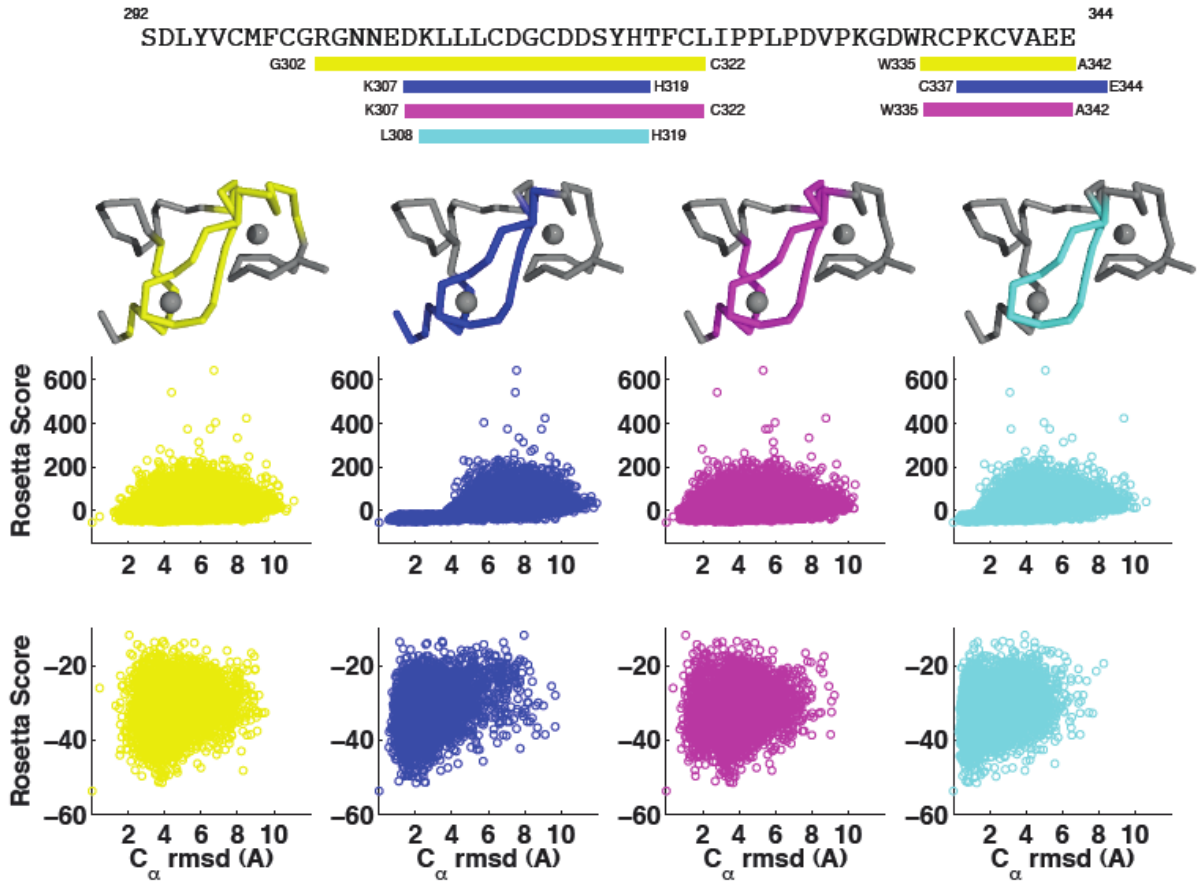

Supplementary Fig. 4 | Score / rmsd for reduced CS-Rosetta models of the apo KDM5A PHD1. Sequence of the KDM5A PHD1 construct used in the NMR experiments is provided as reference for the four different regions considered in recalculation of the score / rmsd plot. These regions are indicated by the colored bars beneath the sequence and are mapped to the ribbon models according to color. In contrast with the all-residue score / rmsd plot in Supplementary Fig. 3, these plots reveal the characteristic funnel shape of convergence, specifically the dark blue region and the cyan region.

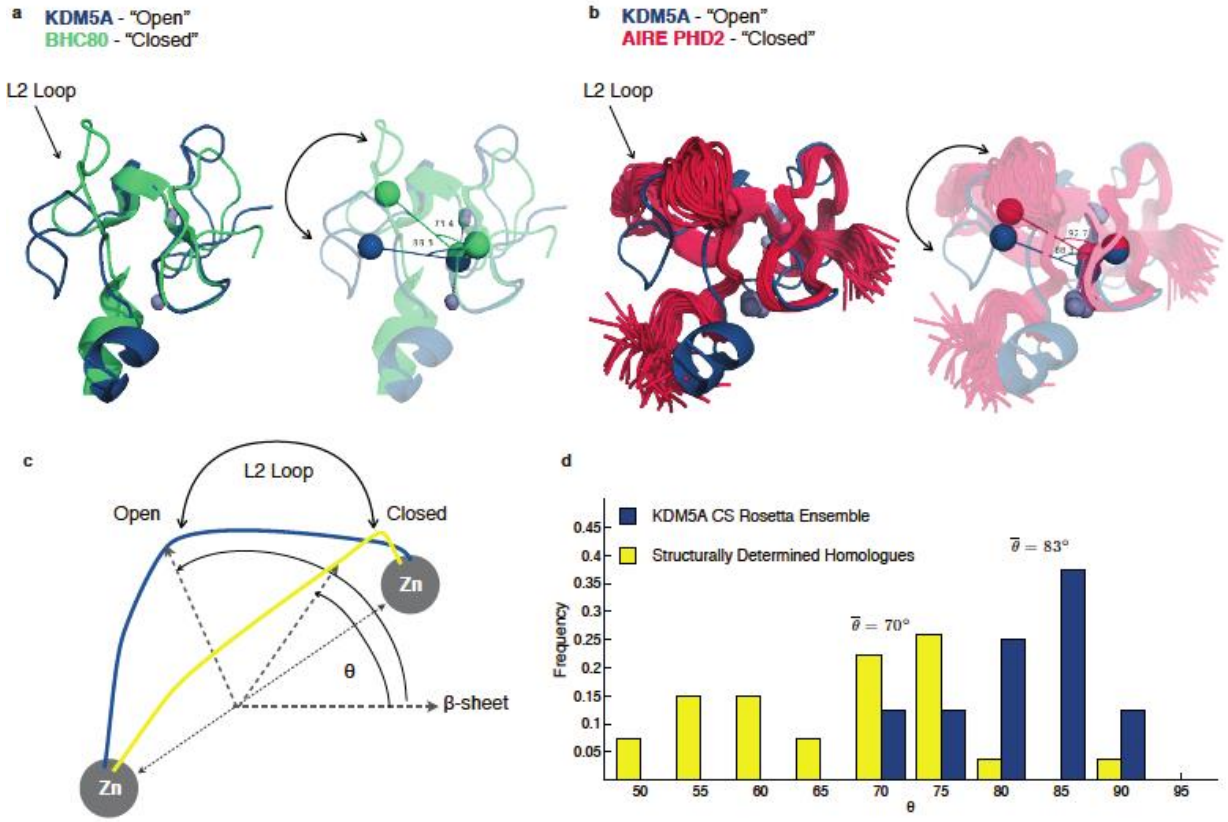

Supplementary Fig. 5 | The L2 loop of KDM5A PHD1 adopts an "open" conformation relative to structurally determined homologous PHD fingers. **.** Superpositions of the CS-Rosetta model of apo KDM5A PHD1 in blue to (**a**) the crystal structure of apo BHC80 in green (PDB: 2PUY, Chain A) and to the (**b**) NMR ensemble (n = 50 models) of AIRE PHD2 (PDB: 2LRI). In the left panels of (**a)** and (**b)**, the position of the L2 Loop is indicated by an arrow and the zinc atoms are shown as spheres. The right panels of (**a)** and (**b)** present a quantitative metric to describe the relative "open"ness of the L2 Loop; here, the individual centers of mass (COMs) for the core β-sheets, the zincs, and the L2 Loop are represented as large spheres colored according to the model. The angle between the COM of the L2 Loop and the COM of structural core is calculated with respect to the COM of the zinc atoms. These angles measure at 88.3°, 73.4° and 92.7°

for KDM5A PHD1, BHC80 and AIRE PHD2, respectively. **(c),** Schematic for quantitation of L2 Loop positioning. Using the COMs for the β-sheet, zinc atoms and L2 Loop, theta (θ) describes the orientation of the L2 Loop with respect to the core of the PHD finger. For small theta, the L2 Loop is well packed against the β-sheet core, and for larger theta, the L2 Loop takes a more extended or "open" conformation. **(d),** Histogram of theta values for 27 structurally determined homologous PHD fingers in yellow and the dihedral restraint filtered CS-Rosetta ensemble (n=8) in blue. The mean theta value for homologous PHD fingers is 70° with a range of 53° to 93°. The CS-Rosetta ensemble is more "open" with a mean theta value of 83° and a range of 70.3° to 90.6°.

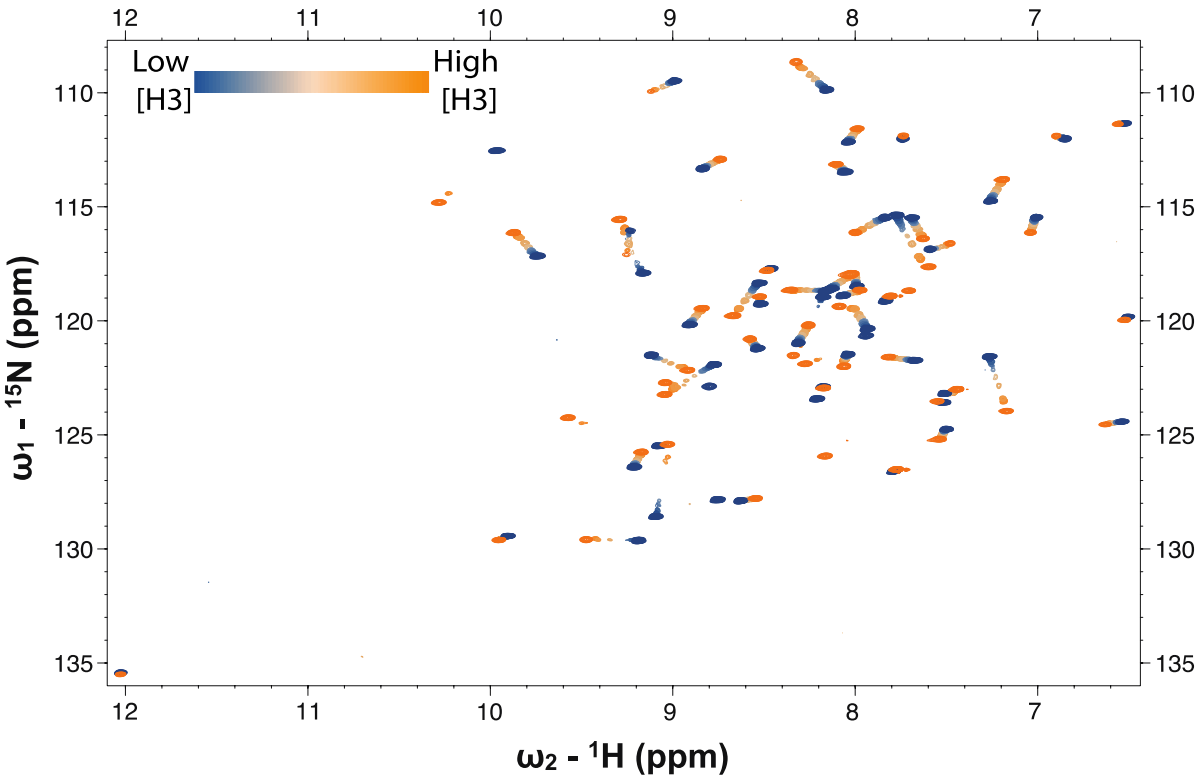

Supplementary Fig. 6 | High-resolution HSQC spectra of the H3-10mer titrations with KDM5A PHD1. Full spectra are presented for the 10 titration points. Spectra are colored according to molar ratio ([H3] / [PHD1]) with blue corresponding to a molar ratio of zero and orange corresponding to a molar ratio of 10. Individual points correspond to molar ratios of 0.2, 0.4, 0.6, 0.8, 1.0, 1.4, 2.4, 4.8 and 10.0.

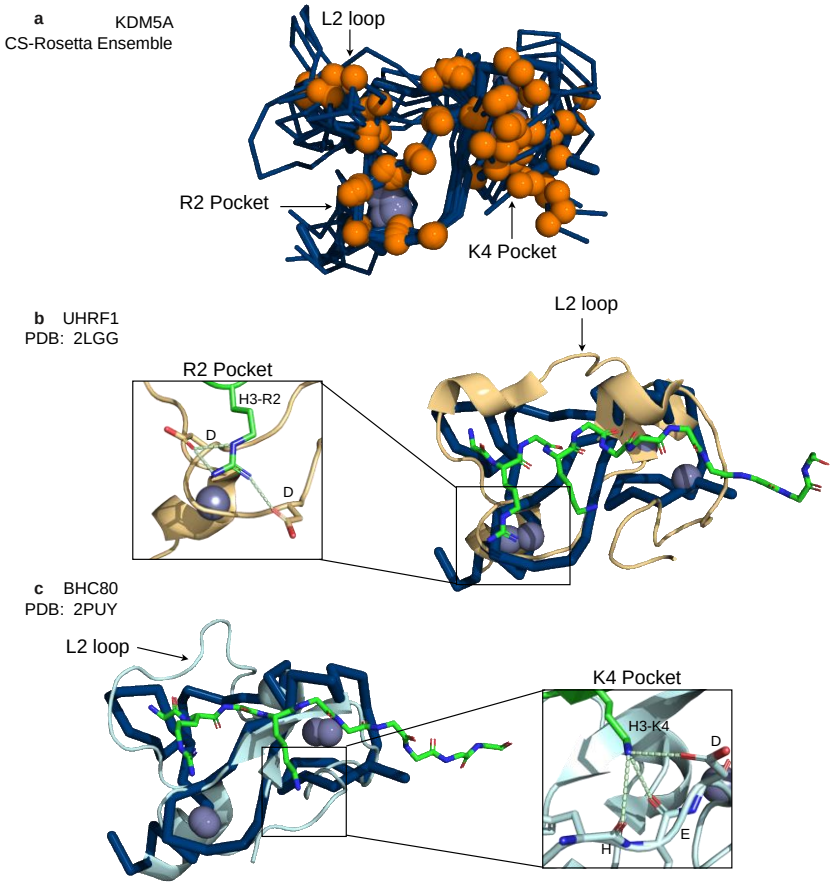

Supplementary Fig. 7 | Structural overlays of KDM5A PHD1 to structurally determined homologous PHD fingers in the H3 bound form. (**A**), The KDM5A ensemble is presented with residues that show significant chemical shifts in the H3 10 mer titration drawn as orange spheres. The primary model of KDM5A (dark blue) overlaid with (**B**), H3-bound form of UHRF1 (light blue) (PDB: 2LGG) and (**C**), bound form of BHC80 (light yellow) (PDB: 2PUY Chain B). These overlays suggest the positioning of the R2 pocket and the K4 pocket.

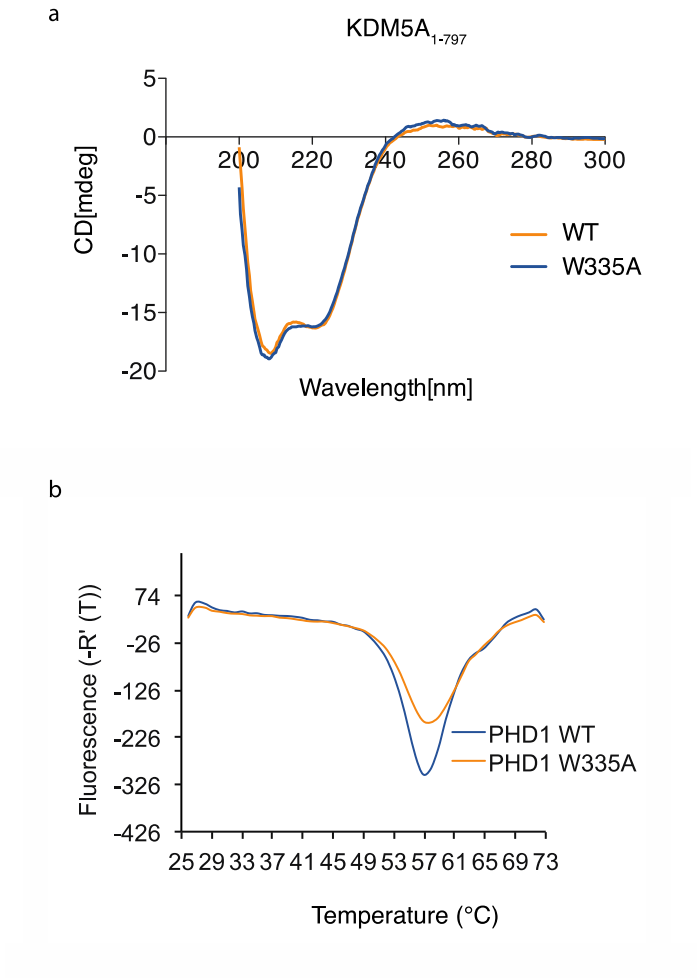

Supplementary Fig. 8 | The overall fold of KDM5A$_{1-797}$ and of its PHD1 alone is not affected by the W335A mutation.

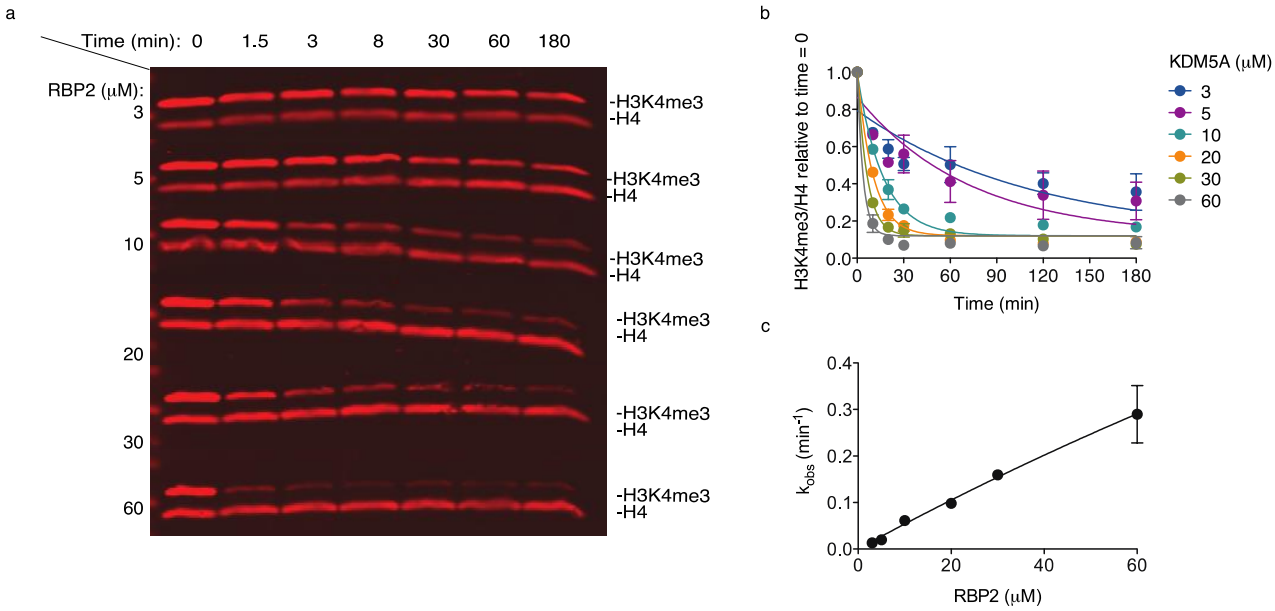

Supplementary Fig. 9 | H3K4me3 nucleosome demethylation by KDM5A under single turnover conditions by quantitative western blot analysis. (**a**) A time-course for demethylation of H3K4me3 nucleosomes (300 nM) by varying concentrations of $KDM5A_{1\text{-}797}$ (3-60 μM), (**b**) Quantification of (a), (**c**) Extrapolation of k_{obs} as a function of $KDM5A_{1\text{-}797}$ concentration. Errors (n = 2) represent s.e.m. Stimulation of nucleosome demethylation (Fig. 4) was performed under subsaturating single turnover conditions due to low affinity of the H3K4me3 nucleosomes for KDM5A.

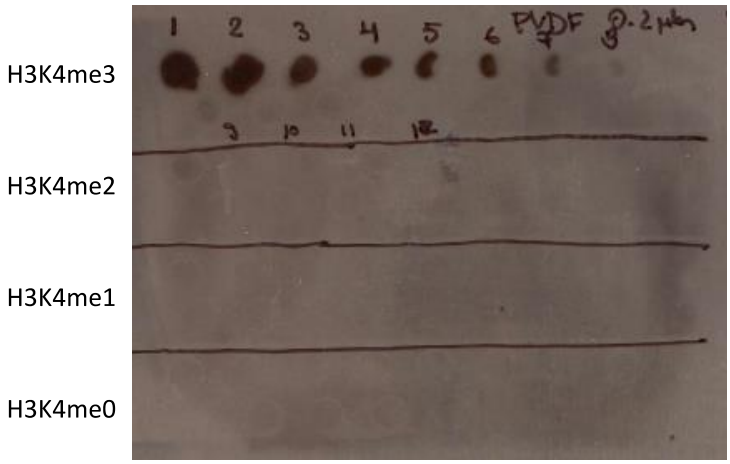

	Amount of H3 peptide (pmol)
1	2000
2	1000
3	500
4	250
5	125
6	62.5
7	31.25
8	15.63
9	7.81
10	3.91
11	1.95
12	0.98

Supplementary Fig. 10 | Specificity of H3K4me3 antibody (Millipore cat # 05-1339). Serial dilution of H3K4me3, me2, me1 and me0 peptide (amino acid 1-18) spotted on a PVDF membrane and probed with anti-H3K4me3 (Millipore cat # 05-1339, 1:2000). The numbers (1-12) on the PVDF membrane represent the picomoles (pmol) of peptide described in the table.

Supplementary Table 1 | Kinetic parameters for the activity of $KDM5A_{1-797}$ and $KDM5A_{1-797}$ W335A on H3K4me3 histone tail peptides. Errors ($n \geq 3$) represent s.e.m.

	KDM5A WT			KDM5A W335A
	H3K4me3	H3K4me2	H3K4me1	H3K4me3
k_{cat} (min^{-1})	2.76 ± 0.05	1.29 ± 0.05	0.66 ± 0.09	1.0 ± 0.1
K_m (μM)	58 ± 5	94 ± 13	204 ± 90	322 ± 99
k_{cat} / K_m (mM^{-1} min^{-1})	48 ± 5	13.7 ± 0.9	3.2 ± 0.2	3 ± 1

Supplementary Table 2 | List of measured HN-HA J-couples for determination of dihedral restraints used in the filtering of CS-Rosetta models.

Spin System	3J [H, H_A] (Hz)
3Leu	7.43608 ± 0.01408
4Tyr	7.22111 ± 0.01209
5Val	9.67294 ± 0.01326
6Cys	4.60161 ± 0.04259
7Met	2.89170 ± 0.04166
8Phe	9.45975 ± 0.01448
9Cys	9.40359 ± 0.01958
11Arg	10.1158 ± 0.01701
13Asn	8.54427 ± 0.05716
14Asn	4.92350 ± 0.52282
15Glu	2.94251 ± 0.14656
16Asp	5.05610 ± 0.05394
17Lys	7.57819 ± 0.01729
18Leu	8.05190 ± 0.03052
19Leu	8.51188 ± 0.02488
20Leu	9.51158 ± 0.01166
21Cys	4.83915 ± 0.04893
22Asp	5.03503 ± 0.03597
24Cys	4.59734 ± 0.02307
25Asp	7.25573 ± 0.02535
26Asp	7.76790 ± 0.10348
27Ser	9.89781 ± 0.02272
28Tyr	9.16404 ± 0.02450
29His	5.64739 ± 0.03682
30Thr	1.57766 ± 0.11407
31Phe	6.40201 ± 0.02824
32Cys	6.00282 ± 0.01367
33Leu	6.81632 ± 0.02679
34Ile	8.39593 ± 0.01624
37Leu	7.60777 ± 0.00908
39Asp	8.53182 ± 0.01219
40Val	5.98469 ± 0.01268
42Lys	7.54778 ± 0.02652
44Asp	6.19144 ± 0.02333
45Trp	8.38952 ± 0.01899
46Arg	9.65188 ± 0.02069
47Cys	3.39969 ± 0.07050
49Lys	7.55272 ± 0.02203
50Cys	7.00092 ± 0.02214
51Val	5.47338 ± 0.01680
52Ala	4.58550 ± 0.01975
53Glu	7.66414 ± 0.01261
54Glu	7.15806 ± 0.00741